Living Radical Photopolymerization Induced Grafting on Thiol–Ene Based Substrates

SIRISH K. REDDY,[1] ROBERT P. SEBRA,[1] KRISTI S. ANSETH,[1,2] CHRISTOPHER N. BOWMAN[1,3]

[1]Department of Chemical and Biological Engineering, University of Colorado, Boulder, Colorado 80309-0424

[2]Howard Hughes Medical Institute, University of Colorado, Boulder, Colorado 80309-0424

[3]Department of Restorative Dentistry, University of Colorado Health Sciences Center, Denver, Colorado 80045-0508

Received 6 December 2004; accepted 6 December 2004
DOI: 10.1002/pola.20693

ABSTRACT: The formation of reactive substrates with iniferter-mediated living radical photopolymerization is a powerful technique for surface modification, which can readily be used to facilitate the incorporation of a variety of surface functionalities. In this research, the photopolymerization kinetics of novel bulk thiol–ene systems have been compared with those of typical acrylate and methacrylate systems when polymerized in the presence of the photoiniferter *p*-xylene bis(*N,N*-diethyl dithiocarbamate) (XDT). In the presence of XDT, the thiol–ene systems photopolymerize more quickly than the traditional acrylate and methacrylate systems by one to two orders of magnitude. Fourier transform infrared spectroscopy has been used to monitor the photografting kinetics of various monomers on dithiocarbamate-functionalized surfaces. Furthermore, this technique has been used to evaluate surface-initiation kinetics and to emphasize the influence of bulk substrate properties on grafting kinetics. Finally, photopatterning has been demonstrated on a dithiocarbamate-incorporated thiol–ene substrate with conventional photolithographic techniques. © 2005 Wiley Periodicals, Inc. J Polym Sci Part A: Polym Chem 43: 2134–2144, 2005
Keywords: living polymerization; photopolymerization; functionalization of polymers

INTRODUCTION

The control of surface chemistry, properties, and interactions has become increasingly important for a wide variety of applications. Surface modification is used to integrate surface functionalities on fabricated device substrates and to enhance numerous properties such as adhesiveness, hydrophobicity, biocompatibility, antifouling, surface hardness, and surface roughness.[1,2] For example, the biocompatibility of biomedical devices or implanted scaffolds is significantly affected by the surface composition and properties. The surface modification of polymeric matrices provides the unique ability to tune and manipulate surface properties without requiring customization of the bulk materials or material properties. Furthermore, surface modification enables the incorporation of multiple surface functionalities, and this is essential for the development and optimal performance of functional devices.

Techniques for surface modification are readily divided into three specific types: physical deposition of surface-active compounds, direct coupling reactions of polymers onto surfaces (grafting-to), and grafting of monomers from reactive surfaces

---

Correspondence to: C. N. Bowman (E-mail: christopher.bowman@colorado.edu)

Journal of Polymer Science: Part A: Polymer Chemistry, Vol. 43, 2134–2144 (2005)

(grafting-from).[3–6] The physical deposition of surface compounds leads to noncovalently bound grafts, and this makes the adsorption a reversible process. Such grafts may be unstable under high shear forces or other adverse chemical and physical conditions. Surface modification via coupling reactions (grafting-to) has several limitations, including incomplete surface coverage, diffusion limitations of the polymers to the surface, and island formation due to steric crowding of the reactive sites by the already grafted polymers. The grafting-from technique, in which grafts are formed through the reaction of monomers from active surfaces, is an attractive alternative for forming robust grafts that provides great control over the density and functionality of the grafts.[3–5]

Current surface modification procedures with the grafting-from approach use techniques such as γ-ray irradiation, UV irradiation, plasma treatment, and glow discharge to create radicals or hydroperoxide groups on surfaces, which facilitate further grafting through radical polymerization at elevated temperatures or upon exposure to UV light.[3,7–9] Each of these approaches involves grafting through radical polymerization, which inherently encompasses uncontrolled reactions such as termination. Well-controlled grafting in precise areas of a device is often required for optimal performance. Improved control of the grafting location, density, and polymer properties is possible with living or controlled radical polymerization grafting schemes, in which the radical concentrations are maintained at a minimum by the equilibration of reactive radicals with their reversibly terminated counterparts.[3,5,10]

Here we focus on quasi living radical photopolymerizations (LRPs) based on dithiocarbamate (DTC)-based photoiniferters, which were pioneered by Otsu.[11,12] Previously, well-defined diblock and triblock copolymers were prepared with this reaction scheme.[13,14] Upon exposure to UV light, the DTC-based iniferters cleave into a reactive carbon-based radical and a less reactive sulfur-based DTC radical. In the presence of monomer A, the reactive radicals initiate a radical polymerization, forming propagating polymer radicals, which, upon end capping with DTC radicals, produce a homopolymer of A. These end-capped, photolabile radicals can recleave upon further absorption of UV light to recover the reactive radical and the DTC radical. This type of reinitiation allows for new monomer B to be sequentially polymerized to the reinitiated polymer ends of A to construct a block copolymer graft of AB. This ability to incorporate distinctly different chemistries in a macromolecule promotes iniferter-based mechanisms for grafting purposes.[3–5,15] Furthermore, the length of grafted chains, spatial resolution, grafting speeds, and grafting density are well controlled with LRP-based reaction schemes.[15–17]

Extensive studies have been conducted on the reaction kinetics of traditional chain-growth systems in the presence of these DTC-based iniferters and the functionalities grafted from these surfaces.[3,12,15,18–21] However, the polymerization kinetics of thiol–ene polymerizations in the presence of DTC groups have not been investigated. Thiol–ene polymerizations are radical, step-growth photopolymerization reactions.[22–25] These reactions have the advantages of traditional acrylate photopolymerization systems, such as ambient curing, rapid polymerization, and solvent-less polymerization, as well as spatial and temporal control over the polymerization. In addition, thiol–ene reactions display unique capabilities such as rapid curing rates in the presence of very little or no photoinitiator and few inhibitory effects of oxygen.[26,27] Furthermore, because of their step-growth mechanism, thiol–ene systems have attractive aspects such as low-volume shrinkage, delayed gelation, and concomitantly low stress development. Features such as these make thiol–ene systems attractive for making microstructured materials.

Thiol–ene polymerization reactions proceed via the sequential propagation of a thiyl radical through a vinyl functional group and subsequent chain transfer of hydrogen from the thiol, which regenerates the thiyl radical.[22–24,28–30] This successive propagation/chain-transfer mechanism is the basis for the step-growth thiol–ene polymerizations and can be presented as follows (k_{pSC} is the kinetic parameter for propagation and k_{CT} is the kinetic parameter for chain train transfer):

$$\text{Propagation } \mathrm{RS}\cdot + \mathrm{R'CH{=}CH_2} \xrightarrow{k_{\mathrm{pSC}}} \mathrm{R'C\cdot H{-}CH_2SR} \quad \text{Step 1}$$

$$\text{Chain Transfer } \mathrm{R'C\cdot H{-}CH_2SR} + \mathrm{RSH} \xrightarrow{k_{\mathrm{CT}}} \mathrm{R'CH_2{-}CH_2SR} + \mathrm{RS}\cdot \quad \text{Step 2}$$

In this article, we investigate the curing kinetics of thiol–ene systems in the presence of photoiniferters and compare their curing rates with those of traditional acrylate and methacrylate systems cured under similar conditions. Surface-initiation kinetics of various substrates prepared in the presence of photolabile DTC groups are also presented. The rapid curing kinetics of thiol–ene systems in the presence of photoiniferters, associated with the attractive curing and polymer aspects of these systems, enables the formation of photopatterned microstructures that are readily surface-modified.

EXPERIMENTAL

Materials

The photoinitiator, 2,2-dimethoxy-2-phenylacetophenone (DMPA), was purchased from Ciba–Geigy (Hawthorne, NY). The photoiniferter, *p*-xylene bis(*N,N*-diethyl dithiocarbamate) (XDT), was donated by 3M. The monomers pentaerythritol tetra(3-mercaptopropionate) (thiol), 1,6-hexanediol diacrylate (HDDA), poly(ethylene glycol) (PEG 375) monoacrylate, triethylene glycol divinyl ether (DVE3), Vectomer 5015 vinyl ether (VE5015), triallyl-1,3,5-triazine-2,4,6-(1H,3H,5H)-trione (triallyl iscocyanurate) (triazine), and trifluoroethyl acrylate were purchased from Aldrich. The monomers triethylene glycol diacrylate (TEGDA) and tetraethylene glycol dimethacrylate (TEGDMA) were purchased from Sartomer. An aromatic urethane diacrylate (Ebecryl 4827) was donated by UCB Chemicals (Smyrna, GA). All monomers, the photoiniferter, and the photoinitiator were used as received.

Instruments

Fourier Transform Infrared (FTIR)

FTIR spectroscopy studies were conducted with a Nicolet 750 Magna FTIR spectrometer with a KBR beam splitter and a deuterated triglycine sulfate detector. Initially, the IR specimen mold containing the sample was placed in a horizontal transmission apparatus, which was continuously purged with dry air. Then, series scans were recorded, with spectra taken at a rate of approximately 2 scans per second. The FTIR experimental setup is described in detail elsewhere.[31] The samples were irradiated until the reaction was complete, as indicated by the functional group absorption spectra no longer decreasing.

Although real-time mid-IR is one of the most commonly employed spectroscopy techniques for following polymerization kinetics, this technique is limited by the sample thickness. However, with the near-IR technique, relatively thick samples can be monitored, as absorption in the near-IR range is fairly low.[32,33] Therefore, the near-IR technique was employed to study the polymerization kinetics of substrate formation and to investigate further the surface-initiation kinetics. The DVE3 and VE5015 conversions were monitored with the carbon–carbon double-bond absorption peak at 6192 cm^{-1}. The TEGDA, TEGDMA, PEG 375 monoacrylate, and HDDA conversions were monitored with the carbon–carbon double-bond peaks at 6164 cm^{-1}. The triflouroethyl acrylate conversions were monitored with double-bond absorption peaks at 6182 cm^{-1}. The conversions were calculated with the ratio of the peak areas before and after photopolymerization.

Furthermore, to investigate the impact of oxygen on the substrate curing kinetics, we spread thin monomer films on an NaCl crystal with a 6-μm wire-wound wet film applicator rod (Paul N. Gardner Co., Inc., Pompano Beach, FL). The polymerization kinetics were monitored with the mid-IR technique. The DVE3 conversion was monitored with the carbon–carbon double-bond peaks at 1619 and 1636 cm^{-1}, and the acrylate conversion was monitored by the monitoring of the double-bond peak at 1636 cm^{-1}.

Illumination Sources

To monitor the photopolymerization kinetics of the monomers with FTIR, we performed the initiation with an EXFO Acticure light source (EXFO, Mississauga, Canada) with a 320–500-nm filter and with the peak emission centered at 365 nm. For micropattern fabrication and for the formation of reactive substrates that were used for measuring the surface kinetics, we employed an optical mask alignment system (Optical Associates, Inc., San Jose, CA) coupled to a 5-cm collimated flood exposure source that generated 45 mW/cm^2 of 365-nm radiation. The irradiation intensities were measured with an International Light (Newburyport, MA) IL1400A radiometer.

Dynamic Mechanical Analysis (DMA)

DMA was used to measure the glass-transition temperatures (T_g's) of the substrates. A sinusoidal stress at a frequency of 1 HZ was applied to the substrate samples to determine the loss tangent as a function of temperature. T_g was defined as the temperature at which the loss tangent peak attained a maximum.

Contact-Angle Measurements

A variety of mono(meth)acrylated functionalities, including PEG 375 monoacrylate and trifluoroethyl acrylate, were photografted onto DTC-incorporated substrates via UV-induced radical photopolymerization. After modification, substrate samples were washed with copious amounts of methanol and water to remove any unreacted monomer. Then, with the sessile drop goniometric technique,[34,35] the contact angles of the modified surfaces were collected in triplicate.

Procedures

Substrate Preparation

The formation of the substrates that were employed to investigate the surface-initiated kinetics and micropattern formation involved the photopolymerization of the base monomer on a clean, transparent glass slide under 5-cm collimated UV light at 45 mW/cm^2. The substrates were polymerized for times that corresponded to the time of the complete reaction, as indicated by FTIR under similar illumination conditions. This reaction involved the photopolymerization of the argon-purged monomers in the presence of either a DTC-based photoiniferter (XDT) or the photoinitiator, DMPA, to form a base layer with either iniferter or no iniferter, respectively. Although the formation of the acrylate substrates involved the polymerization of acrylic monomers, the preparation of the thiol–ene substrates involved the polymerization of stoichiometric ratios of thiol and ene monomers. Contact photolithographic methods were used to photopolymerize the base layers onto glass slides. The polymerized base substrates were washed thoroughly with methanol and water to remove any unreacted monomer material.[36]

IR Mold Preparation and Investigation of Surface-Initiated Kinetics

The IR specimen mold was prepared with the previously described substrate-coated glass slide and a clean glass slide, with a metal spacer between them. The mold was clamped together, and the monomer solution was carefully pipetted from the open sides of the specimen mold to avoid bubble formation. Furthermore, metal spacers (50, 100, and 200 μm thick) were used to control the thickness of the monomer solution on top of the substrate. The surface-initiation kinetics of the monomer solutions were monitored with near-FTIR. The monomer solutions employed for the investigation of the surface-initiation kinetics were purified and further purged with argon, but the FTIR chamber was only purged with dry air.

Micropattern Formation

Photoiniferters based on DTC groups were used to form photoreactive surfaces, which were then employed to form photopatterned surfaces. The monomer systems composed of either thiol–ene monomers or acrylate monomers were cured in the presence of an iniferter (XDT) to form an iniferter-incorporated matrix, as shown in Scheme 1. The substrates were then washed with deionized water and methanol before being coated with a monomer. Photolithography, exploiting selective exposure to UV light through a photomask, was used to form micropatterns grafted on the reactive surfaces. Micropatterning photolithography was performed with an optical mask alignment system, and the experimental procedure is described in detail elsewhere.[37] Upon illumination with UV light, the DTC moieties that were attached to the substrate cleaved and provided surface-attached active carbon-based radicals and propagating inactive DTC radicals. In the presence of a vinyl-terminated grafting monomer, these carbon-based radicals propagated and reversibly end-capped with DTC radicals to form surface-tethered polymer chains. For monoacrylates, the graft length was controlled by the exposure time, and this further enhanced the degree of surface-graft control.

RESULTS AND DISCUSSION

Formation of the Reactive Substrates: Thiol–Ene Systems versus Acrylate Systems

The formation of DTC-containing reactive surfaces is a powerful route for LRP-based surface modification, and this technique has been used for a wide variety of vinyl monomers. However, this technique is limited by the extremely slow photopolymerization rates of current monomer systems.[19,20] Experiments were conducted to investigate the curing kinetics of several thiol–ene systems in the presence of XDT (DTC precursor) and

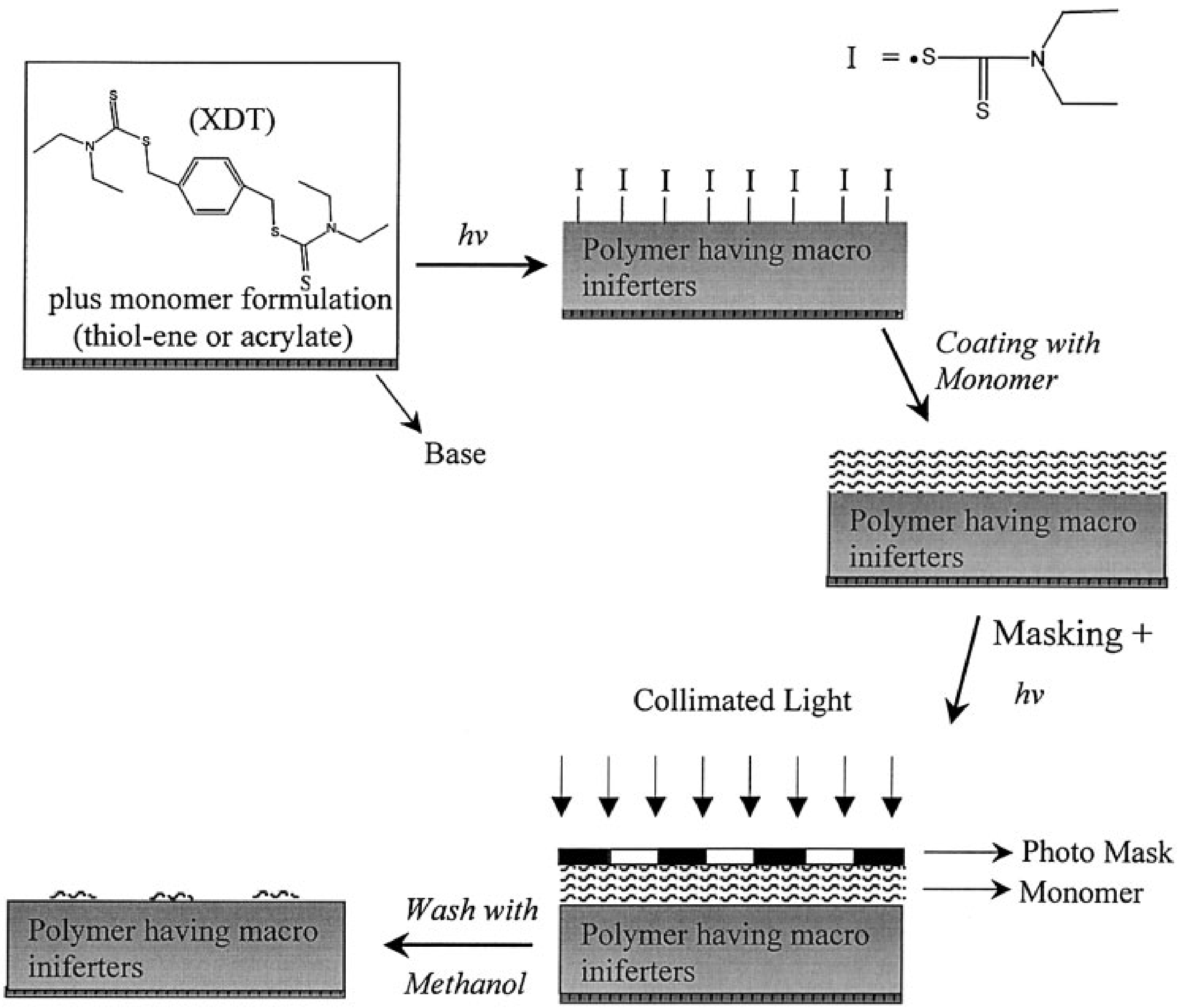

Scheme 1. Chemistry used to functionalize acrylate and thiol–ene surfaces with various grafting monomers.

were compared with those of typical acrylate and methacrylate systems cured under similar conditions. Specifically, polymerization kinetics are presented for two thiol–ene systems: thiol–DVE3 and thiol–VE5015. The acrylate and methacrylate systems were TEGDA and TEGDMA, respectively. Figure 1(a) plots experimentally observed (FTIR) polymerization kinetics of the thiol–DVE3, thiol–VE5015, acrylate, and methacrylate systems in the presence of 0.5 wt % XDT and at an irradiation intensity of 5 mW/cm^2. The polymerization kinetic data from Figure 1(a) are further represented in Figure 1(b) to present the polymerization rates as a function of conversion. In the presence of XDT, the thiol–ene systems photopolymerize more quickly than the traditional acrylate and methacrylate systems by one to two orders of magnitude [Fig. 1(b)]. The great difference in the curing speeds of the thiol–ene and acrylate and methacrylate systems in the presence of XDT is comparable to the difference in the reactivity of these systems in the presence of conventional photoinitiators. Furthermore, although the thiol–ene systems achieve almost complete conversion, the acrylate (TEGDA) and methacrylate (TEGDMA) systems show lower final conversions of 80 and 65%, respectively. The observed low conversions of the acrylate and methacrylate systems, in the presence of XDT, are consistent with reported final conversion values of several similar systems.[19,20] High conversions achievable through the thiol–ene mechanism, coupled with its characteristic step-growth behavior, result in systems with a significantly reduced concentration of leachable, residual, uncured monomers. This reduction is pertinent be-

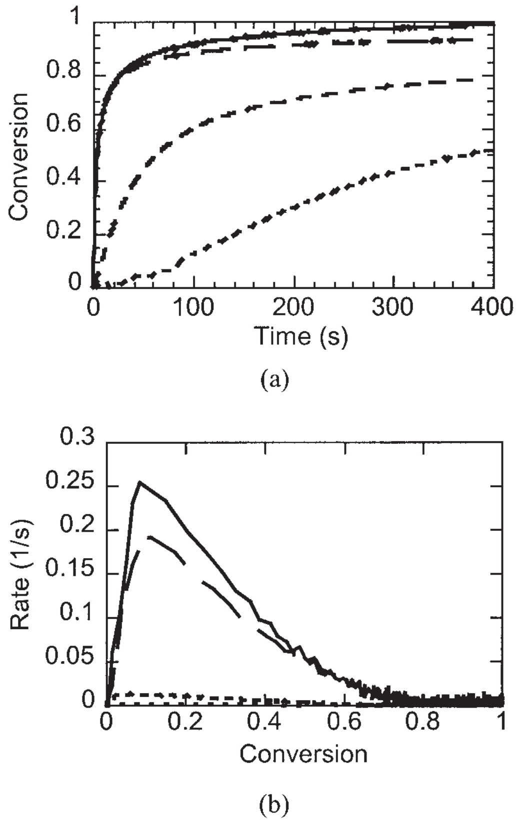

(a)

(b)

Figure 1. Comparison of (a) the conversion as a function of time and (b) the polymerization rate as a function of conversion of thiol–ene systems with those of typical acrylate and methacrylate systems in the presence of the 0.5 wt % photoiniferter (XDT): (—) thiol–DVE3, (— —) thiol–VE5015, (– –) TEGDA, and (- - -) TEGDMA. All polymerizations were conducted at an intensity of 5 mW/cm^2.

cause uncured monomers often limit device applicability because of compatibility and mechanical failure. Specifically, for applications in which cells are in contact with the material, leachable monomers frequently lead to necrosis. The high polymerization rates of thiol–ene systems in the presence of iniferters, such as XDT, present a novel route to the rapid formation of substrates with controlled shape and structures while enabling subsequent surface modification.

Thiol–ene photopolymerizations also offer extensive versatility in their chemistries.[38] A wide variety of vinyl and thiol chemistries are radically curable via a thiol–ene mechanism, and this imparts specific chemical and physical properties to the final cured product. These chemistries allow for a wide range of network properties, ranging from rubbery to glassy materials. For example, a thiol–DVE3 system forms a rubbery substrate with a T_g of −20 °C, whereas a thiol–triazine substrate forms a glassy polymer with a T_g of 48 °C. T_g's of these substrates were found with DMA. The unique advantages of thiol–ene curable systems, coupled with their chemical versatility, make them attractive for various applications.

Furthermore, these systems are insensitive to oxygen inhibition and, therefore, have a distinct advantage over typical acrylate systems. Figure 2 presents conversion–time profiles for the polymerization of thiol–DVE3 and TEGDA systems containing 0.5 wt % XDT in the presence of air. Although the thiol–ene system cures rapidly even in the presence of air, the TEGDA system shows a significantly reduced conversion under these conditions.

Kinetics of Surface Grafting and Micropatterning

The polymerization kinetics, initiated by surface-tethered iniferters, were studied with near-IR spectroscopy. Figure 3 shows the conversion profiles of a trifluoroethyl acrylate monomer grafted on thiol–VE5015 substrates prepared without XDT and with 2 wt % XDT. The conversion–time profiles of trifluoroethyl acrylate show that there is no significant polymerization or grafting on a substrate that is prepared in the presence of the DMPA photoinitiator (0.5 wt %) in the absence of XDT. The plot also indicates that the trifluoroethyl acrylate monomer graft-polymerizes readily on a substrate prepared in the presence of XDT,

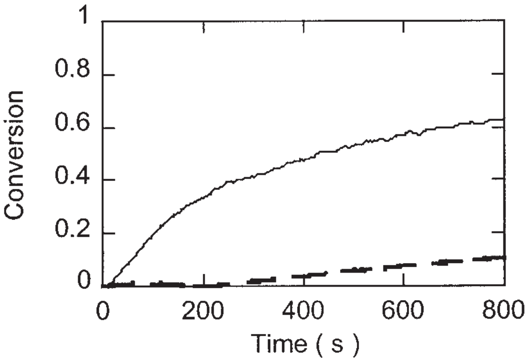

Figure 2. Conversion–time profiles of nonlaminated thiol–ene and acrylate systems cured in the presence of air: (—) thiol–DVE3 (thiol–ene system) and (– –) TEGDA (acrylate system). Both samples were cured in the presence of the 0.5 wt % photoiniferter and were polymerized at an intensity of 5 mW/cm^2.

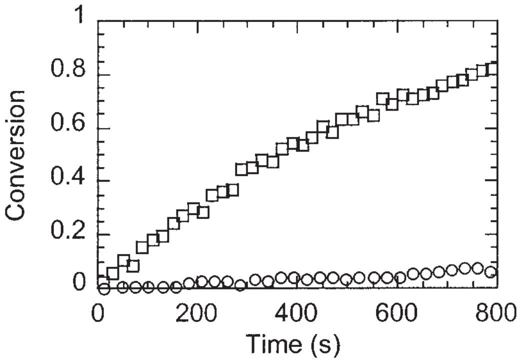

Figure 3. Conversion kinetics of the triflouroethyl acrylate monomer grafted onto substrates prepared (□) in the presence of photoiniferter XDT and (○) in the absence of XDT but in the presence of traditional photoinitiator DMPA. The triflouroethyl acrylate was polymerized on the substrate surfaces without additional photoinitiator at an intensity of 40 mW/cm^2. The substrates were formed by the polymerization of thiol–VE5015. The amounts of the triflouroethyl acrylate monomer on the substrates corresponded to a thickness of 50 μm.

demonstrating the surface-initiating capabilities of the DTC groups incorporated into the substrates.

Figure 4(a) plots the conversion of the trifluoroethyl acrylate monomer (graftable monomer) on a thiol–VE5015 substrate prepared in the presence of 2 wt % XDT for two different amounts of the graftable monomer on the substrate corresponding to thicknesses of 50 and 200 μm. The plot clearly indicates that the monomer conversion rate is dependent on the amount of the graftable monomer on the substrate. This phenomenon of thickness-dependent conversion is in direct contrast to what is expected from the kinetics of bulk-initiated systems. However, for surface-initiated polymerizations, the relative monomer conversion rates are expected to be dependent on the monomer thickness as the absolute polymerization does not change. Hence, the monomer conversion rate (i.e., that normalized by the total amount of the monomer) should vary inversely with the monomer thickness. The inverse thickness dependence of the monomer conversion rate was investigated by the normalization of the monomer conversion [Fig. 4(a)] with respect to the corresponding initial monomer thicknesses. We obtained normalized conversions by keeping the conversion of the 50-μm-thick monomer layer unchanged and normalizing the 200-μm-thick monomer conversion by multiplying the monomer conversion by a factor of four. A plot of the normalized conversion versus time [Fig. 4(b)] reveals that these normalized conversions overlay for small conversions, thereby confirming the surface-initiated nature of the polymerization. However, these conversions do not overlay for higher conversions (>35%), and this can likely be explained by the effects of chain transfer, irreversible termination, and a small amount of bulk, initiator-less polymerization induced by the longer time exposure.

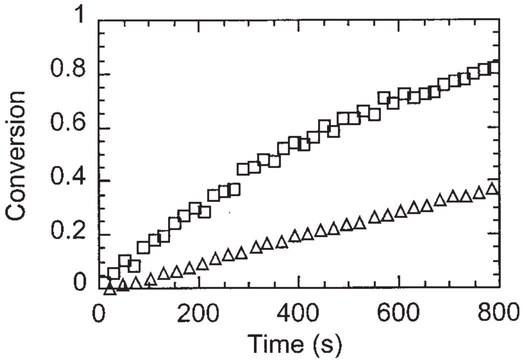

(a)

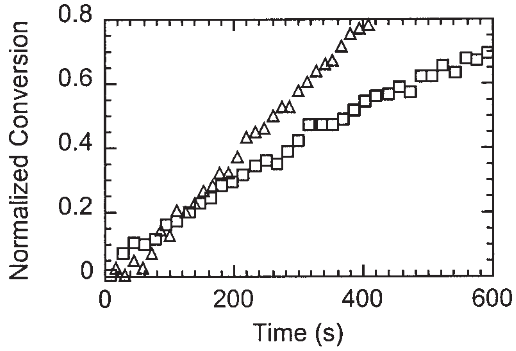

(b)

Figure 4. (a) Conversion kinetics for two different thicknesses of the triflouroethyl acrylate monomer on substrates polymerized in the presence of the 2 wt % photoiniferter (XDT) and (b) normalization of the same conversions to account for the thickness and total monomer amount. For the normalization, the conversion kinetics of the thinner sample (thickness = 50 μm) were left unchanged, whereas those of the thicker sample (thickness = 200 μm) were scaled by the thickness ratio. The monomer was cured on the surfaces without additional photoinitiator and was illuminated at an intensity of 40 mW/cm^2. The data are from samples with a monomer thickness of (△) 200 or (□) 50 μm. The surfaces were prepared from stoichiometric ratios of thiol and VE5015.

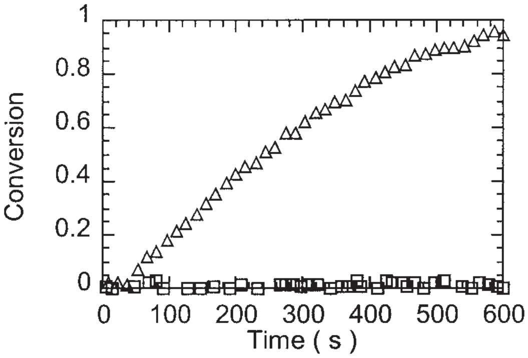

(a)

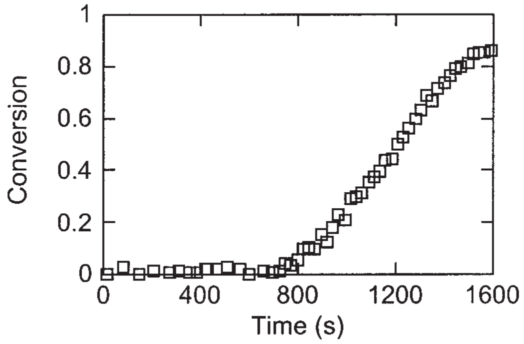

(b)

Figure 5. (a) Comparison of the conversion kinetics of PEG 375 monoacrylate polymerized on substrates prepared (△) in the presence of 2 wt % XDT and (□) in the presence of 2 wt % DMPA (but in the absence of XDT). The substrates were formed by the photopolymerization of thiol and triazine monomers. (b) Monomer conversion, monitored over an extended period, on a substrate made in the absence of photoiniferter XDT. The monomer was polymerized on the surfaces without additional photoinitiator and at an intensity of 40 mW/cm^2. The amounts of the PEG 375 monoacrylate monomer on the substrate corresponded to a thickness of 100 μm.

Figure 5(a) compares the conversion kinetics of PEG 375 monoacrylate on a thiol–triazine substrate prepared in the presence of XDT with the conversion kinetics on a thiol–triazine substrate prepared in the presence of the conventional DMPA photoinitiator (but in the absence of XDT). Although the monomer does not photopolymerize on a substrate that is prepared in the absence of XDT, it readily graft-polymerizes on a substrate containing DTC groups. The conversions of the PEG 375 monoacrylate monomer on a thiol–triazine substrate polymerized in the absence of added XDT, from Figure 5(a), are presented for extended exposure times in Figure 5(b). This plot shows that although the monomers on the substrates prepared in the presence of the DMPA photoinitiator do not show any apparent polymerization at reduced exposure times, polymerization occurs readily for prolonged exposure times. Furthermore, curing studies of PEG 375 monoacrylate between two glass slides (results not shown here) indicate that the monomer is not capable of undergoing polymerization under these irradiation conditions, even after extended periods of irradiation (up to 60 min). This aspect of polymerization, in which the monomer does not undergo polymerization on glass substrates but polymerizes on the polymer base substrate in the absence of DTC functionality, might be attributed to monomer diffusion into the polymer base substrate and polymerization induced by unreacted DMPA in the base substrate or diffusing into the bulk material.

The ability to control the graft density of a modified surface is recognized as an important factor for controlling the surface properties of a material. Figure 6 indicates that altering the XDT concentration used to polymerize the substrate is useful in controlling the grafting density. PEG 375 monoacrylate exhibits a lower polymerization rate on substrates polymerized with a lower XDT concentration (0.5 wt %) than on substrates prepared with relatively high iniferter concentrations (2 wt %). The higher polymerization rates suggest that the grafting density is also higher. Furthermore, the inhibition time that oc-

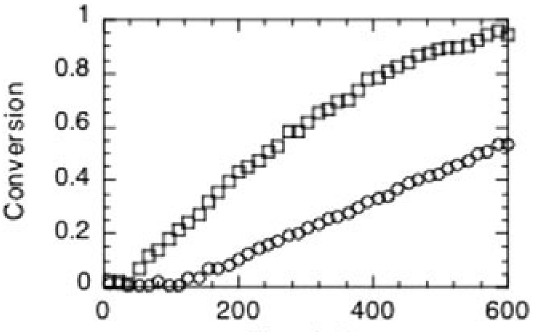

Figure 6. Comparison of the conversion kinetics of PEG 375 monoacrylate polymerized on substrates made in the presence of (○) 0.5 and (□) 2 wt % XDT. The substrates were formed by the photopolymerization of thiol and triazine monomers. The monomer, PEG 375 monoacrylate, was cured on the substrate without additional photoinitiator and was illuminated at an intensity of 40 mW/cm^2.

curs before substantial graft formation is reduced for grafting on substrates that contain elevated DTC concentrations.

To investigate the influence of the substrate materials' properties on their grafting characteristics, we performed grafting studies on a substrate material, the thiol–DVE3 substrate, which is relatively rubbery in comparison with previously considered substrate materials, such as the thiol–triazine and thiol–VE5015 substrates. Figure 7 presents the grafting kinetics of monomer HDDA on a thiol–DVE3 substrate prepared in the presence of either XDT or DMPA. It also presents the curing kinetics of HDDA between two glass slides. Although HDDA does not undergo any substantial polymerization between glass slides, it readily polymerizes on the thiol–DVE3 substrates prepared in the presence and absence of XDT. The curing kinetics of HDDA between two glass slides clearly show that the monomer is incapable of undergoing homopolymerization under these irradiation conditions. This result further indicates that the polymerization of HDDA on the thiol–DVE3 substrate containing no DTC groups may be due to monomer diffusion into the rubbery thiol–DVE3 substrates and to polymerization due to unreacted DMPA in the base substrate. Furthermore, although HDDA cures on a thiol–DVE3 substrate made in the absence of XDT, it does not polymerize (results not shown) on a relatively glassy substrate, thiol–VE5015, polymerized under similar conditions, and this indicates that the material properties of the substrate are important in determining the surface polymerization characteristics.

Furthermore, a comparison of the polymerization kinetics of HDDA on thiol–DVE substrates made in the presence and absence of XDT indicates that the HDDA monomer achieves higher final conversions on thiol–DVE3 substrates that do not contain any DTC groups than on substrates that contain DTC groups. These plots also show that HDDA starts polymerizing earlier on substrates that have DTC groups incorporated into them. The reduced inhibition time in the polymerization of the monomer on surfaces with DTC groups is due to the DTC-based surface-initiation process, in contrast to slower diffusion and initiation with unreacted DMPA on a substrate made in the absence of XDT. The lower final conversion of HDDA on substrates containing DTC groups can be attributed to the cleaving of DTC groups (from substrate materials), which, when present in HDDA, reduce the radical concentration in the bulk HDDA monomer because of the reversible termination. This behavior is in agreement with previous work,[19] in which the polymerization of the bulk monomer with photoiniferters led to a lower final conversion than that with the conventional photoinitiator DMPA.

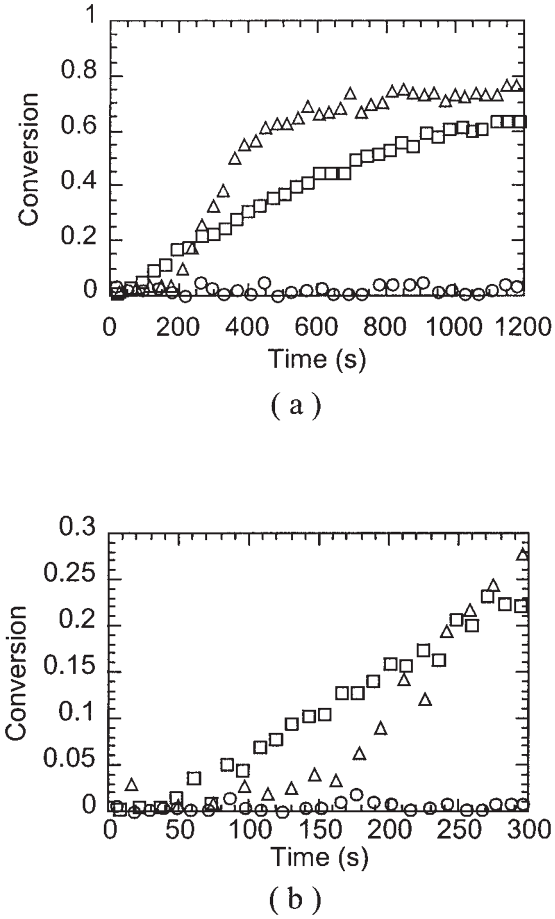

Figure 7. (a) Comparison of the conversion kinetics of HDDA polymerized on three different substrates. The monomer conversion is shown as a function of time (□) on a thiol–DVE3 substrate prepared in the presence of the 2 wt % photoiniferter (XDT), (△) on a thiol–DVE3 substrate polymerized in the presence of 2 wt % DMPA and in the absence of the photoiniferter, and (○) on glass. (b) The same conversion plotted for the initial 300 s. The HDDA monomer was polymerized on the surfaces without additional photoinitiator and was illuminated at an intensity of 40 mW/cm^2. The amounts of the HDDA monomer on the substrates corresponded to a thickness of 100 μm.

Experiments were conducted to compare the surface-grafting kinetics of XDT-containing thiol–ene substrates and acrylate substrates. Figure 8 compares the grafting kinetics of PEG 375 monoacrylate on a thiol–ene (thiol–triazine) substrate

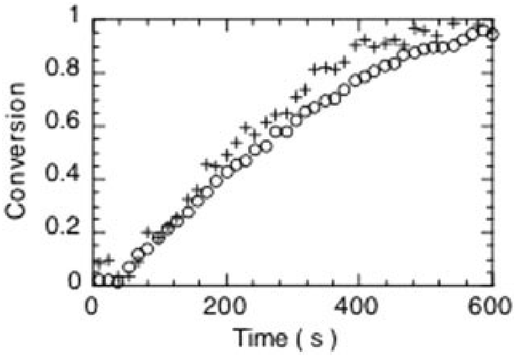

Figure 8. Comparison of the conversion kinetics of monomer PEG 375 on (○) thiol–triazine and (+) urethane diacrylate/TEGDA substrates, both made in the presence of 2 wt % XDT. The monomer PEG 375 was cured on the surfaces without additional photoinitiator and was illuminated at an intensity of 40 mW/cm^2.

with those of PEG 375 monoacrylate on a urethane diacrylate/TEGDA substrate. Both the thiol–ene and the urethane diacrylate/TEGDA substrates were prepared in the presence of 2 wt % XDT. The conversion–time profiles indicate that the PEG 375 monoacrylate grafts at a similar rate on the thiol–ene and acrylate substrates. This result shows that the two substrates exhibit very similar grafting capabilities, despite being formed with very different reaction mechanisms (thiol–ene substrates with a step-growth mechanism and acrylate with a chain-growth mechanism). This indicates a great similarity in their fundamental polymerization schemes in the presence of photoiniferters such as XDT.

Photopatterning with the XDT-based LRP mechanism is presented in Figure 9; 25-mm^2 regions of PEG 375 monoacrylate were photografted on a thiol–triazine substrate containing 0.5 wt % XDT. After rinsing with methanol and water, the PEG 375 grafted regions were stained red with hematoxylin to contrast the ungrafted substrate (clear) and the surface-grafted pattern (stained in red). This sample was exposed to 45 mW/cm^2 light for 800 s with photolithographic techniques to ensure that grafting had occurred only in the exposed regions. Furthermore, the contact angle of the grafted areas was approximately 10° with conventional goniometry, which contrasted with the substrate contact angle of 45°. A similar photolithographic technique was used to modify DTC-incorporated thiol–triazine surfaces via photografting with trifluoroethyl acrylate, and this resulted in a hydrophobic surface with a contact angle of 80°.

CONCLUSIONS

With the DTC-mediated LRP chemistry demonstrated in this research, various surface chemistries have been obtained simply by proper monomer selection. A variety of grafted chemistries have been demonstrated, ranging from hydrophilic PEG 375 monoacrylate modified surfaces with a contact angle of 10° to hydrophobic surface modification with trifluoroethyl acrylate, which yields a contact angle of 80°.

The thiol–ene systems, which rapidly polymerize with DTC-incorporated iniferters, provide a route for the rapid fabrication of iniferter-incorporated surfaces that are readily surface-modified. Furthermore, thiol–ene chemistries offer a wide versatility for substrate materials, thus providing an opportunity for choosing materials with desired bulk properties. For example, the thiol–DVE3 substrate has a T_g of −20 °C, whereas the T_g's of the thiol–VE5015 and thiol–triazine substrates are 5 and 48 °C, respectively. Furthermore, as discussed previously, the mechanical properties of the base material appear to play an important role in determining whether surface modification occurs because of grafting or because of the apparent diffusion of unreacted initiators and graftable monomer.

Exploiting surface-attached DTC groups to initiate the growth of controlled polymer chains from a substrate is useful in tailoring chemical and biological surface interactions. Applications requiring controlled cell adhesion, hydrophobic–hydrophilic interactions, protein attachment, drug delivery, sensory responses, or surface fluo-

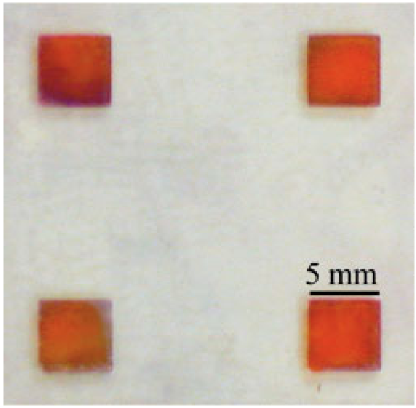

Figure 9. Thiol–triazine substrate sample photografted with PEG 375 monoacrylate for 900 s. The PEG 375 grafted regions were stained red by hematoxylin.

rescence, among others, all benefit from this chemistry. Photolithographically controlled grafting enables the patterning of multiple surface chemistries and hence facilitates spatial and temporal control over surface properties. Although this research has successfully demonstrated that thiol–ene systems can be rapidly polymerized in the presence of XDT to form reactive substrates for surface modification, further work has to be performed to acquire a fundamental understanding of the various DTC adduct products formed in these polymerizations.

The authors are grateful for the financial support of this research from the Defense Advanced Research Projects Agency Symbiosys program, Air Force Office of Scientific Research, the National Science Foundation (DMR-9796100), and a National Science Foundation Tie Grant (0120943). S. K. Reddy and R. P. Sebra were also supported by a fellowship from the U.S. Department of Education Graduate Assistance in Areas of National Need program.

REFERENCES AND NOTES

1. Higashi, J.; Nakayama, Y.; Marchant, R. E.; Matsuda, T. Langmuir 1999, 15, 2080–2088.
2. Nakayama, Y.; Anderson, J. M.; Matsuda, T. J Biomed Mater Res 2000, 53, 584–591.
3. Luo, N.; Metters, A. T.; Hutchison, J. B.; Bowman, C. N.; Anseth, K. S. Macromolecules 2003, 36, 6739–6745.
4. Luo, N.; Hutchison, J. B.; Anseth, K. S.; Bowman, C. N. Macromolecules 2002, 35, 2487–2493.
5. Luo, N.; Hutchison, J. B.; Anseth, K. S.; Bowman, C. N. J Polym Sci Part A: Polym Chem 2002, 40, 1885–1891.
6. Ma, M. H.; Davis, R. H.; Bowman, C. N. Macromolecules 2000, 33, 331–335.
7. Arnold, J. C.; Sawin, H. H. J Appl Phys 1991, 70, 5314–5317.
8. Flamm, D. L. Solid State Technol 1991, 34, 105–105.
9. Wang, H.; Brown, H. R. J Polym Sci Part A: Polym Chem 2004, 42, 253–262.
10. Feng, W.; Brash, J.; Zhu, S. J Polym Sci Part A: Polym Chem 2004, 42, 2931–2942.
11. Otsu, T.; Yoshida, M. Makromol Chem Rapid Commun 1982, 3, 127–132.
12. Otsu, T. J Polym Sci Part A: Polym Chem 2000, 38, 2121–2136.
13. Otsu, T.; Kuriyama, A. Polym J 1985, 17, 97–104.
14. Kroeze, E.; de Boer, B.; ten Brinke, G.; Hadziioannou, G. Macromolecules 1996, 29, 8599–8605.
15. Nakayama, Y.; Matsuda, T. Macromolecules 1996, 29, 8622–8630.
16. de Boer, B.; Simon, H. K.; Werts, M. P. L.; van der Vegte, E. W.; Hadziioannou, G. Macromolecules 2000, 33, 349–356.
17. Lee, H. J.; Nakayama, Y.; Matsuda, T. Macromolecules 1999, 32, 6989–6995.
18. Nakayama, Y.; Matsuda, T. Macromolecules 1999, 32, 5405–5410.
19. Kannurpatti, A. R.; Lu, S. X.; Bunker, G. M.; Bowman, C. N. Macromolecules 1996, 29, 7310–7315.
20. Ward, J. H.; Shahar, A.; Peppas, N. A. Polymer 2002, 43, 1745–1752.
21. Kannurpatti, A. R.; Goodner, M. D.; Lee, H. R.; Bowman, C. N. ACS Symp Ser 1997, 673, 51–62.
22. Kharasch, M. S.; Nudenberg, W.; Mantell, G. J. J Org Chem 1951, 16, 524.
23. Morgan, C. R.; Magnotta, F.; Ketley, A. D. J Polym Sci Part A: Polym Chem 1977, 15, 627–645.
24. Cramer, N. B.; Bowman, C. N. J Polym Sci Part A: Polym Chem 2001, 39, 3311–3319.
25. Reddy, S. K.; Cramer, N. B.; O'Brien, A. K.; Cross, T.; Raj, R.; Bowman, C. N. Macromol Symp 2004, 206, 361–374.
26. Cramer, N. B.; Scott, J. P.; Bowman, C. N. Macromolecules 2002, 35, 5361–5365.
27. Reddy, S. K.; Cramer, N. B.; Cross, T.; Raj, R.; Bowman, C. N. Chem Mater 2003, 15, 4257–4261.
28. Jacobine, A. F.; Glaser, D. M.; Grabek, P. J.; Mancini, D.; Masterson, M.; Nakos, S. T.; Rakas, M. A.; Woods, J. G. J Appl Polym Sci 1992, 45, 471–485.
29. Lee, T. Y.; Kaung, W.; Jonsson, S.; Lowery, K.; Guymon, C. A.; Hoyle, C. E. J Polym Sci Part A: Polym Chem 2004, 42, 4424–4436.
30. Cramer, N. B.; Reddy, S. K.; Lu, H.; Cross, T.; Raj, R.; Bowman, C. N. J Polym Sci Part A: Polym Chem 2004, 42, 1752–1757.
31. Berchtold, K. A.; Bowman, C. N. RadTech Eur Conf Proc 1999, 767.
32. Stansbury, J. W.; Dickens, S. H. Dent Mater 2001, 17, 71–79.
33. Lovell, L. G.; Lu, H.; Elliott, J. E.; Stansbury, J. W.; Bowman, C. N. Dent Mater 2001, 17, 504–511.
34. Cassie, A. B. D. Discuss Faraday Soc 1952, 75, 5041.
35. Brain, C.; Whitesides, G. A. Langmuir 1989, 5, 1370–1378.
36. Haraldsson, K. T.; Hutchison, J. B.; Sebra, R. P.; Good, B. T.; Anseth, K. S.; Bowman, C. N. 3D Polymeric Microfluidic Device Fabrication via Contact Liquid Photolithographic Polymerization (CLiPP); Sensors and Actuators Part B: Chemical (under review).
37. Hutchison, J. B.; Haraldsson, K. T.; Good, B. T.; Sebra, R. P.; Luo, N.; Anseth, K. S.; Bowman, C. N. Robust Polymer Microfluidic Device Fabrication via Contact Liquid Photolithographic Polymerization (CLiPP) LAB ON A CHIP (6):658–662 2004.
38. Hoyle, C. E.; Cole, M. C.; Bachemin, M. A.; Yoder, B.; Nguyen, C. K.; Kuang, W.; Viswanathan, K.; Bowman, C. N.; Cramer, N. B.; Jonsson, S. RadTech Asia Tech Proc 2000, 211.